DESIGN AND PERMANENT MAGNETS REDUCTION OF LINEAR OSCILLATORY MACHINE FOR RECIPROCATING DRIVES IN TRANSPORT

Matúš Horník[1,*], Pavol Rafajdus[1], Hao Chen[2], Yassen Gorbounov[3], Gojko Joksimović[4]

[1]University of Zilina, Department of Power System and Electric Drives, Zilina, Slovakia
[2]China University of Mining and Technology, School of Electrical Engineering, Xuzhou, China
[3]New Bulgarian University, Department of Informatics, Sofia, Bulgaria
[4]University of Montenegro, Faculty of Electrical Engineering, Podgorica, Montenegro

*E-mail of corresponding author: matus.hornik@feit.uniza.sk

Matúš Horník 0009-0008-0885-5704,
Yassen Gorbounov 0000-0002-2936-951X,
Pavol Rafajdus 0000-0003-2903-3394,
Gojko Joksimović 0000-0002-2764-1540

Resume

Electric vehicles (EVs) require efficient compressors for air-conditioning and battery thermal management, typically driven by a dedicated electric motor. In this paper is dealt with the design and optimization of a stator-magnet transverse-flux linear oscillatory machine (SMTLOM) intended for such compressor applications. The topology employs permanent magnets embedded in the stator, enabling simplified assembly, improved vibration robustness, and reduced dependence on rare-earth materials. A detailed 3D finite element analysis was conducted to maximize the performance, while minimizing the volume of permanent magnets. The results demonstrate the feasibility of SMTLOM for EV compressor drives and highlight the trade-offs between force capability, efficiency, and magnet usage.

Article info

Received 12 February 2026
Accepted 28 March 2026
Online 17 April 2026

Keywords:

Linear compressor
electric vehicle
stator-magnet moving-iron
transversal-flux linear machine
three-dimensional finite-element analysis
dual-mode current excitation
rare-earth magnet reduction
force profile optimization

ISSN 1335-4205 (print version)
ISSN 2585-7878 (online version)

Available online: https://doi.org/10.26552/com.C.2026.024

1 Introduction

With climate changes and environmental pollution becoming more critical than ever, the electric vehicles (EVs) offer possibilities of more eco-friendly transportation solution. Electric vehicles are already used a lot in transportation, though the research on them is far from over. Their efficiency and driving range are the biggest focus. By optimizing components used in the EVs it is possible to make them more appealing for the world. One such component used in every type of EV are the compressors. They are mainly used in air conditioning units and battery thermal management systems. Research in [1] provided a review on air conditioning systems (ACS) used in electric vehicles. In the EVs, the AC unit is separately supplied in contrast to the combusting engine vehicles. A separate electric motor is needed for their operation. As is mentioned in [2], the ACS have high power consumption in EVs. This is affected by weather conditions as well and in winter when the ACS can have the biggest power consumption in vehicles. In most cases rotational electric motors are used, for their simple design as can be seen in [3-4]. This leads to a necessary transmission from rotary motion of electric motor to linear motion of the piston in the ACS. Therefore, a direct linear motion without the transmission would be preferable for transmission losses reduction.

Linear oscillatory machines (LOMs) have been the cornerstone of numerous industrial applications due to their ability to directly convert electromagnetic forces into linear motion without the need for mechanical transmissions and are particularly advantageous in scenarios where oscillatory motion with high efficiency is required. Therefore, their usage in compressor applications is possible, and they are already being used in this field, such as in [5].

Nowadays the transfer flux linear oscillatory

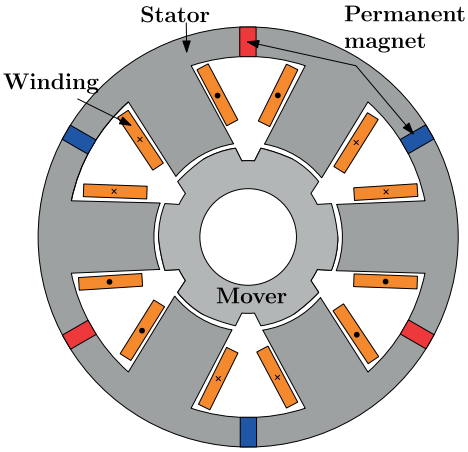

Figure 1 *Radial cross section of SMTLOM*

Table 1 *Specific maximum parameters of SMTLOM*

Description	Parameter	Value	Unit
Voltage RMS	V	145	[V]
Current RMS	I	0.3&1.7	[A]
Frequency	f	75	[Hz]
Total Width	W	60	[mm]
Stator Diameter	D_{so}	120	[mm]
Mover Diameter	D_{si}	46	[mm]

machine with permanent magnets (PMs) on the mover are the most used type [6]. Those machines are highly efficient, with high power density. However, they suffer on the reliability side. Since their magnets are placed on the moving part, the magnets are susceptible to vibration and high temperatures. Thus, to evade some of these deficiencies, similar machine with PMs on the stator was introduced by Boldea [7] to improve the motor reliability. This model was later modified to a stator-magnet transverse-flux linear oscillatory machine (SMTLOM) in [8-9], to keep the reliability and boost the efficiency of the machine. By moving the PMs to the outer part of the stator, the magnets can be better cooled, and easier to install.

The main contribution of this paper is the systematic reduction of stator-mounted rare-earth magnet volume in an SMTLOM, while maintaining the full-stroke force coverage for EV compressor applications.

2 Design requirements and specifications

As it is demonstrated in Figure 1, the SMTLOM was selected for the present study. The machine contains magnets embedded in the stator yoke. The incorporation of rare-earth permanent magnets (PM) composed of NdFeB within the stator yoke confers two primary advantages: facilitation of installation and replacement of the PM, and enhancement of protection against vibrations induced by the mover.

The incorporation of the PM modifies the flux path configuration, transitioning frosm a series to a parallel structure. Consequently, this approach results in a substantial reduction in the PM usage. The SMTLOM is operated with twin stators that generate magnetomotive forces (MMFs) when energized by current. These MMFs interact with the permanent magnet's field, creating a flux imbalance that drives the mover toward the stator with higher flux density. The machine's operation is facilitated by single-phase sinusoidal currents, thereby generating an oscillatory magnetic field that drives the mover axially. This resonant motion, synchronized with the power supply frequency, facilitates precise oscillatory motion, which is well-suited for applications such as compressors.

For the design of the SMTLOM, several key parameters must be defined, as this forms the initial step in the development of any electric machine. The requirements and constraints applied in this work are summarised in Table 1. These values were selected to ensure that the proposed SMTLOM is suitable for use in compressor applications.

According to the operating principle of the SMTLOM, described in the previous section, the machine performs an oscillatory motion whose frequency corresponds to the frequency of the applied voltage. The relationship is expressed as:

$$v_m = l_{st} f \,, \tag{1}$$

where v_m denotes the linear velocity of the mover, l_{st} represents the full bidirectional stroke length, and f

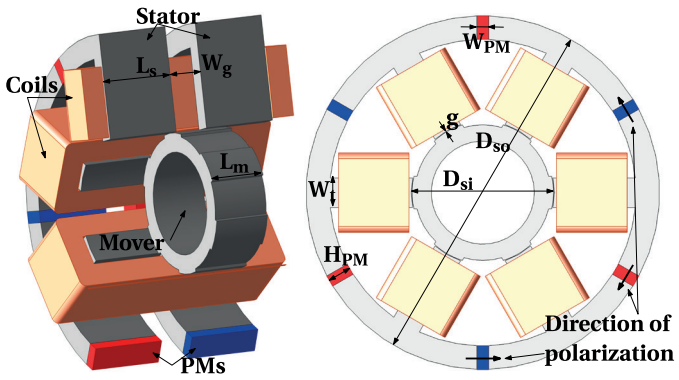

Figure 2 *Illustration of the front view of the SMTLOM and its partial section without the mechanical springs*

is the excitation frequency. This expression does not consider the effects of mechanical springs. The stroke length is particularly important, as it directly influences the mover velocity and consequently affects the overall performance of the compressor.

2.1 Influence of stroke length

The stroke length has a substantial influence on both the performance and energy demand of a linear compressor. A longer stroke enables a larger volume change inside the compression chamber, which allows the system to reach higher pressures and achieve greater compression ratios. However, an extended stroke must be controlled with high precision, as excessive displacement may result in over-compression and reduced efficiency. In contrast, a shorter stroke requires the machine to operate at a higher number of cycles to reach the same pressure level, increasing the mechanical wear and overall energy consumption.

2.2 Force and current requirement

In linear compressor operation, the piston is driven by a linear electric actuator and oscillates directly along a single axis, eliminating the need for a crankshaft mechanism. As a result, the electromagnetic force and phase current vary significantly between the compression and decompression strokes. During the compression, a considerable amount of force is necessary to counteract the resistance of the working fluid and the existing chamber backpressure. Although the decompression typically demands less force, additional thrust may still be required to overcome the stiffness of mechanical springs. Rapid switching between the two phases calls for brief periods of increased current to accelerate or decelerate the mover. Mechanical springs help to reduce the required electrical current during these transitions, increasing system efficiency.

For this reason, a dual-mode current strategy is implemented. Figure 2 illustrates the SMTLOM geometry and the principal parameters included in the design.

2.3 Low-current and high-current modes

In the low-current operation, hereafter referred to as the efficiency mode, the system operates with minimal electrical input, maintaining oscillations close to their natural resonance. This operational mode is suitable for maintaining system pressure under light load. By delivering only the current necessary to offset mechanical losses such as friction and damping, the mover can oscillate with very low energy consumption. This reduces mechanical and thermal stress, prolongs the service life, and ensures that the transition to high-current operation can be performed immediately when required.

The high-current operation, hereafter referred to as the power mode, is engaged when the compressor must deliver significantly higher force, for instance when facing elevated backpressure, compressing liquid refrigerant, or achieving higher compression ratios. Increasing the supplied current strengthens the magnetomotive force in the armature winding and thus raises the electromagnetic thrust required for demanding operating points. One practical approach for switching between the current modes is modifying the electrical properties of the armature winding through the use of a tapped winding structure.

Both operational modes, efficiency and power, are incorporated into the SMTLOM design to ensure optimal force generation in dependence on the compressor's mechanical requirements. The detailed specifications for each mode are given in Table 1.

3 Reference force determination

Before optimizing the linear oscillatory motor, it is necessary to determine the required mechanical force that the motor must generate during operation. In this section, therefore, the focus is not on the motor itself, but

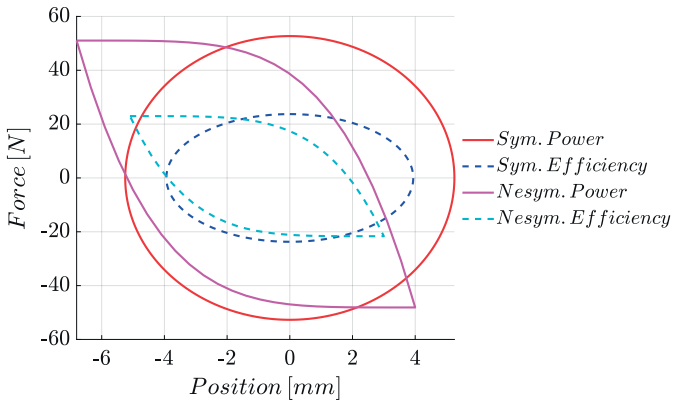

Figure 3 *Theoretical forces required from electric motor in compressor*

on the mechanical load it must drive - the reciprocating compressor of the cooling system. It is described how the target force profiles used in the optimization of the linear oscillatory machine were derived. Such a force can be seen in Figure 3.

By analyzing the gas pressure difference acting on the piston and the resulting displacement, the corresponding force profile $F(x)$ required to perform the compression and suction strokes can be obtained. This force profile serves as the design target for the electromagnetic optimization of the motor, ensuring that the motor produces sufficient thrust over the entire motion range while maintaining efficiency. Two main models were used: a non-symmetric profile that emulates the real pressure behavior in the compressor, and a symmetric (pressure-based) profile that corresponds to idealized sinusoidal operation. The non-symmetric formulation allows to reproduce the different compression and expansion forces that occur in the reciprocating cycle.

3.1 Non-symmetric force model

The non-symmetric force profile $F(x)$ is described by a nonlinear interpolation law using an exponent α_{ns}. It provides an adjustable shape that can be tuned to reproduce realistic asymmetric compression behavior.

The extended range of piston displacement can be defined as:

$$x_{\min,ext} = x_{\min} - \Delta_{ext}, \tag{2}$$

$$x_{\max,ext} = x_{\max} + \Delta_{ext}, \tag{3}$$

$$L = x_{\max,ext} - x_{\min,ext}, \tag{4}$$

where $x_{\min}$ and $x_{\max}$ represent the nominal stroke limits, and Δ_{ext} slightly enlarges this range to ensure that boundary effects are included during optimization. This prevents numerical clipping when generating the full cycle trajectory.

The interpolation shape is defined as:

$$s(x) = \left(\frac{x - x_{\min}}{L}\right)^{\alpha_{ns}}. \tag{5}$$

The interpolation function $s(x)$ is defined over the displacement interval $x \in [x_{\min,ext}, x_{\max,ext}]$, with $\alpha_{ns} > 0$ being a shape exponent controlling the degree of force asymmetry. In Figure 3 the $\alpha_{ns} = 4.5$.

The actual force function is:

$$F(x) = F_{\max} + (F_{\min} - F_{\max})s(x). \tag{6}$$

Alternatively:

$$F(x) = (1 - s(x))F_{\max} + s(x)F_{\min}. \tag{7}$$

To determine $F_{\max}$ and $F_{\min}$, two target points are used:

$$(x_1, F_1), (x_2, F_2). \tag{8}$$

Then, one can calculate:

$$s_1 = s(x_1), s_2 = s(x_2). \tag{9}$$

Substituting the calculated interpolation values s_1 and s_2 into the force expression leads to the following linear system:

$$\begin{bmatrix} 1 - s_1 & s_1 \\ 1 - s_2 & s_2 \end{bmatrix} \begin{bmatrix} F_{\max} \\ F_{\min} \end{bmatrix} = \begin{bmatrix} F_1 \\ F_2 \end{bmatrix}. \tag{10}$$

The solutions are:

$$F_{\max} = \frac{F_1 s_2 - F_2 s_1}{s_2 - s_1}, \tag{11}$$

$$F_{\min} = \frac{F_2(1 - s_1) - F_1(1 - s_2)}{s_2 - s_1}. \tag{12}$$

These equations provide explicit values for the maximum and minimum forces of the nonlinear asymmetric curve. They are used to generate the complete forward and backward motion profiles for dynamic analysis.

Table 2 *Properties of NdFeB PM at 25°C*

Parameter	Value	Unit
H_{cj}	1592	kA/m
H_c	901	kA/m
B_r	1.35	T

3.2 Symmetric pressure-based model

For comparison, a symmetric sinusoidal model is developed based purely on the pressure difference acting on the piston. This model represents the ideal power mode of the compressor, where the compression and expansion are balanced.

The piston area is:

$$A = \pi\left(\frac{D_{pist}}{2}\right)^2. \tag{13}$$

The theoretical maximum force:

$$F_{\max} = \Delta p \cdot A \cdot reserve\,. \tag{14}$$

To model the efficiency mode, reduced amplitude values are introduced:

$$F_{\max,ext} = \eta_F F_{\max}\,, \tag{15}$$

$$x_{\max,ext} = \eta_x x_{\max}\,. \tag{16}$$

Assuming sinusoidal motion at frequency f:

$$x_{power}(t) = x_{\max,ext}\sin(2\pi ft), \tag{17}$$

$$F_{power}(t) = F_{\max,ext}\cos(2\pi ft). \tag{18}$$

Efficiency mode is:

$$x_{eff}(t) = x_{\max,ext}\sin(2\pi ft), \tag{19}$$

$$F_{eff}(t) = F_{\max,ext}\cos(2\pi ft). \tag{20}$$

These sinusoidal expressions are used for reference simulations and energy evaluation.

3.3 Scaling of the non-symmetric profile to efficiency mode

To combine both models:

$$x_{ns,eff}(t) = \eta_x x_{ns}(t), \tag{21}$$

$$F_{ns,eff}(t) = \eta_F F_{ns}(t). \tag{22}$$

This preserves the shape of the asymmetric force curve while reducing its amplitude and stroke. Such scaling enables direct comparison of realistic and idealized excitation modes under identical frequency conditions.

4 Design priorities

As can be seen in Figure 3, the force is in fact required during the whole stroke and not just at a peak. Any further optimization of the proposed machine will reflect this. To know what parameters to focus on, it is important to set goals for the optimization. As there is more than one requirement, it is also good to set priorities among them. For that purpose, a list of requirements is compiled:

1. Achievement of forces in Efficiency and Power modes,
2. Adherence to the dimensions,
3. Reduction of rare-earth materials in magnets,
4. Efficiency above 92% in efficiency mode.

As mentioned before, the force must be applied throughout the entire stroke, or at least the majority of it, to ensure sufficient power for compression and decompression. As the Power mode is easier to achieve thanks to the higher current and because efficiency is not required, the optimization can focus on Efficiency mode. As mentioned in the previous section, a positive change in efficiency mode force also has a positive effect on Power mode.

Adherence to the dimensions is important, as the entire motor must fit within the compressor system. If this requirement is not met, the linear motor cannot be used for the compressor, which requires the force specified above. The maximum width of the machine cannot exceed 60 mm, not including the winding, and the diameter cannot exceed 120 mm.

Reducing rare-earth magnets is important due to their high costs, limited supply, and environmental impact. Where possible, they can be replaced with more abundant alternatives, such as ferrites.

The compressor should work continuously to maintain resonance, even when cooling is not exactly necessary. In this case, the linear motor is required to be highly efficient. Therefore, a required efficiency at least 92% was set. The referred efficiency applies only to the linear electric machine and not to the entire system.

To optimize the model, a replica of the model created by the Chinese scientists was utilized [8]. The current was selected to be 0.3 A for Efficiency mode and 1.7 A for Power mode. The NdFeB permanent magnet parameters are given in Table 2.

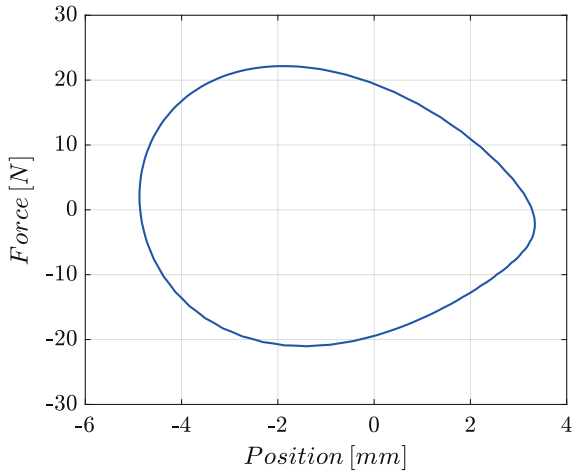

Figure 4 *Required reference force in Efficiency mode*

The coercivity H_c is the magnetic field strength at which the magnetic flux density B becomes zero, while the intrinsic coercivity H_{cj} corresponds to the field at which the magnetic polarization J (or magnetization M) vanishes. Unlike H_c, which is affected by demagnetizing effects, H_{cj} directly indicates the resistance of a permanent magnet to irreversible demagnetization.

All the possible modifications and curves with which the optimisation was conducted are depicted in Figure 3. It has been established that any alterations made to the Efficiency mode would be reflected in the Power mode, due to the work that had been completed during research. It was therefore determined that the Efficiency mode should be prioritised as the most significant, based on that, in this mode, efficiency was deemed to be a prerequisite. The reference Efficiency mode curve is presented in Figure 4. This curve was obtained through collaboration with an industrial partner, BSH Drives and Pumps s.r.o., utilising the theoretical equations, and reflects the reality to a greater extent than curves in Figure 3.

It is imperative to note that, given the utilisation of this curve as a point of reference, a comparison of the simulation results against it is essential. The objective is to attain a force that is greater throughout the entirety of the movement, or that encompasses the majority of the curve.

5 Methods used for optimization

For the optimization, Parametric and Mixed-Integer Sequential Quadratic Programming (Gradient and Discrete Optimization) methods were employed. Both optimization strategies are integrated within the Ansys Maxwell 3D simulation environment, enabling automated design exploration and performance improvement of electromagnetic systems. To establish a basis for comparison, the simulated force was evaluated in relation to the reference curve.

The Parametric optimization approach involves systematical varying selected design parameters - such as geometric dimensions, material properties, or excitation values to evaluate their influence on key performance metrics. By defining those parameters as variables within the simulation model, Ansys Maxwell can automatically perform parametric sweeps or response surface optimizations, allowing the identification of optimal configurations and sensitivity relationships between input parameters and output performance. This method provides a clear understanding of how each variable affects the overall machine behavior, facilitating efficient design refinement.

The Mixed-Integer Sequential Quadratic Programming (MISQP) method, on the other hand, extends the traditional gradient-based Sequential Quadratic Programming (SQP) by incorporating discrete or integer variables. The algorithm iteratively solves a series of quadratic programming subproblems that approximate the nonlinear objective function and constraints using gradient and Hessian information. While continuous variables are optimized through the gradient-based search, the discrete variables are handled via branch-and-bound or enumeration techniques. This hybrid structure enables simultaneous optimization of both continuous and discrete design variables such as slot numbers, magnet arrangements, or dimensional parameters resulting in a globally efficient and physically feasible design solution.

6 Optimization of the stator-magnet transverse flux linear oscillatory machine

A final dimensional model was selected from the set of simulated models. The parameters of the final dimension are delineated in Table 3. Given these parameters, the stator-magnet transverse flux linear oscillatory machine is consistent with the maximum dimensional requirements for its diameter, width, and inner space in the mover, thereby allowing for the accommodation of a piston.

Table 3 *Dimensions of the chosen SMTLOM*

Variable Name	Parameter	Value
Mover width	L_m	24 mm
Mover diameter	D_{si}	39.6 mm
Mover inside diameter	D_{in}	31 mm
Mover tooth height	H_{Mt}	5 mm
Mover tooth width	L_{Mt}	19.7 mm
Mover tooth depth	W_{Mt}	15 mm
Stator diameter	D_{so}	120 mm
Stator width	L_s	24 mm
Stator tooth height	H_t	33.7 mm
Stator tooth width	W_t	19.7 mm
Stator air gap	W_g	6 mm
Air gap	g	0.3 mm
PM height	H_{PM}	13 mm

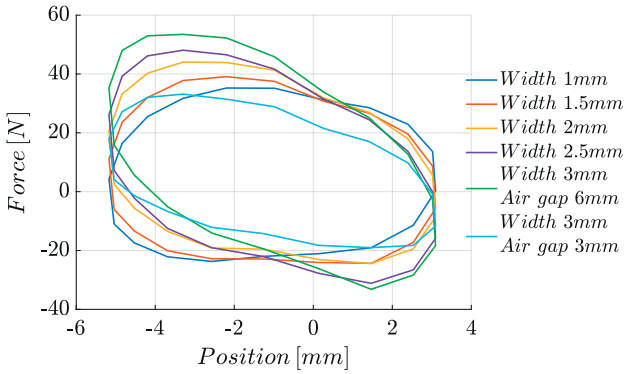

Figure 5 *Force-position characteristics for different permanent magnet widths in efficiency mode*

The first step is to find a model which will produce desired force curve during the whole operation of the SMTLOM. Therefore a machine was simulated with a width of magnet of 3 mm. This was done for two different stator air gaps of 3 mm and 6 mm. As previously mentioned these changes lead to a different distribution of forces during movement. In Figure 5, these curves can be observed, along with further magnet reduction, which was done at stator air gap of 6 mm, as it provided higher forces during the complete movement, compared to 3 mm stator air gap.

Upon examination of the Figure 5, two notable facts emerge. The initial observation is that an increased quantity of NdFeB magnets results in a higher peak force. The latter is of utmost importance for the optimization. As is evident from the maximum and minimum values observed at the limit point of the position axis, this effect is not without its drawbacks for the model in question.

At this point, the electric motor reaches its maximum mobility limit, leading to a change in direction. The force that would be optimal is then opposite to the force it was producing during movement in the previous direction. When comparing the obtained force result, it is not sufficient to consider only the peak.

As demonstrated by Figure 5, it is evident that increasing the width of the magnet results in higher force amplitudes in both directions of motion. This behavior is characteristic of configurations with a stronger magnetic flux, as a larger volume of magnetic material enables the machine to generate higher peak attractive and repulsive forces. However, as the width of the magnet increases, the symmetry of the force with respect to the zero level on the force axis becomes significantly worse. The initial oval shape of the curves gradually becomes distorted, resulting in a narrower and less balanced appearance.

This imbalance signifies that the force exerted on the mover is not uniformly distributed over the entire stroke. In the context of linear compressor applications, force symmetry is of paramount importance. An asymmetric force profile has the potential to exert a negative influence on the dynamics and the overall energy efficiency of the drive. As demonstrated in Figure 4, the force should be symmetrical about the zero level of the Y-axis. Consequently, configurations with reduced magnet widths, which exhibit enhanced symmetry even at decreased amplitudes, are more appropriate for meeting the compressor requirements.

Given the extensive array of simulations conducted, a precise selection process was imperative. For the purpose of comparison, a comparison of simulated results and theoretical force was conducted.

7 Comparison of simulation results to theoretical forces

As previously indicated, the selection of the appropriate model was conducted by a comprehensive consideration of the entire moving process. A comparative analysis was conducted among numerous models.

Given the movement's bidirectional nature, both the simulated and theoretical curves were divided according to the movement direction. The theoretical force is divided into two components: one that is directed forward and one that is directed backward. This approach was similarly implemented in the context of the simulated models in Figure 6, where the number in the legend is the width of the magnets.

The segmentation was performed at the extreme mover positions, where the direction changes. Since the theoretical force curve contained more data points than the simulated results, interpolation was used to align both datasets. The simulation step size was relatively large due to computational limits, which caused visibly discrete force points and required smoothing.

A common position vector x_{common} was created over the overlapping region of both datasets, and all the curves were linearly interpolated onto this grid. This ensured a direct point-wise comparison, while avoiding nonphysical extrapolation. Invalid or incomplete simulation curves were automatically skipped.

The comparison evaluated the percentage of the stroke where the simulated force magnitude exceeded

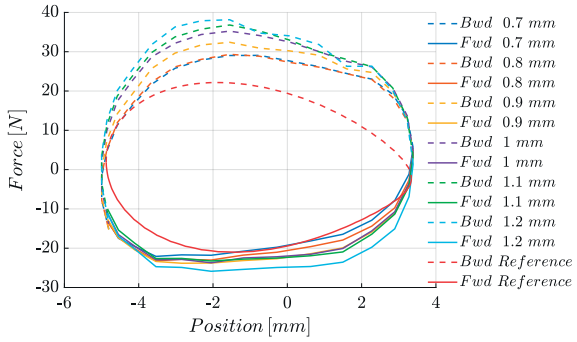

Figure 6 *Force-position characteristics for different permanent magnet widths including the reference model*

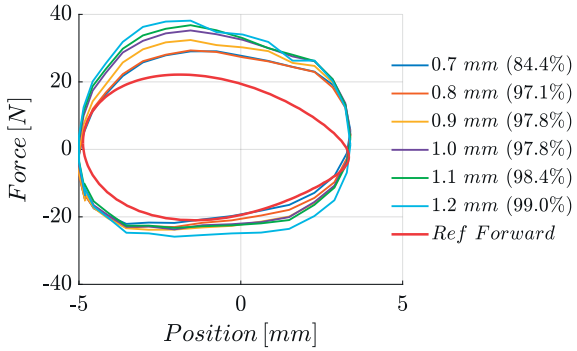

Figure 7 *Forces comparison of efficiency mode*

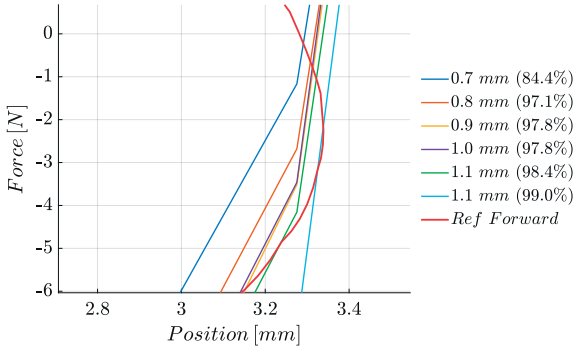

Figure 8 *Forces coparison at maximum movement of the piston of efficiency mode*

the theoretical reference. The resulting values, shown in Figure 7, indicate that magnet widths below 1.2 mm lead to a rapid drop in performance. A 99 % match is considered sufficient, as interpolation was involved. The detail in Figure 8 shows a small region where the simulated force did not fully cover the theoretical curve, likely due to coarse simulation resolution. The chosen model was therefore selected as the most suitable candidate for further detailed evaluation.

8 Final results of optimized linear motor

The final model of the SMTLOM, shown in Figure 2, was chosen and its parameters are listed in Table 4. As described in the previous sections, this model fulfils the dimensional goal, the force requirement, explained in section 2, and the reduction of rare-earth magnets that has been done in section 6. Only the efficiency goal remains unknown.

Table 4 *Dimensions of the final SMTLOM model*

Variable Name	Label	Value
Mover width	L_m	24 mm
Mover diameter	D_{si}	39.6 mm
Mover diameter inside	D_{in}	31 mm
Mover tooth height	H_{Mt}	5 mm
Mover tooth width	L_{Mt}	19.7 mm
Mover tooth depth	W_{Mt}	15 mm
Stator diameter	D_{so}	120 mm
Stator width	L_s	24 mm
Stator tooth height	H_t	33.7 mm
Stator tooth width	W_t	19.7 mm
Stator air gap	W_g	6 mm
Air gap	g	0.3 mm
PM height	H_{PM}	13 mm
PM width	W_{PM}	1.2 mm

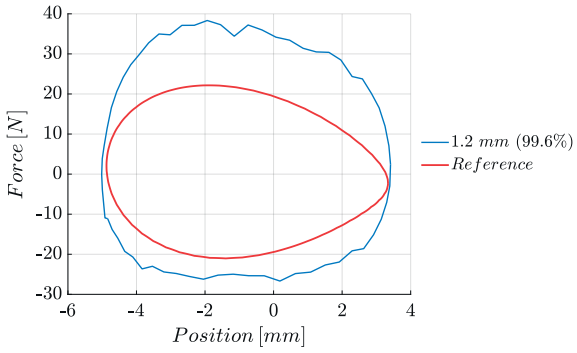

Figure 9 *Efficiency mode force curve of the final model*

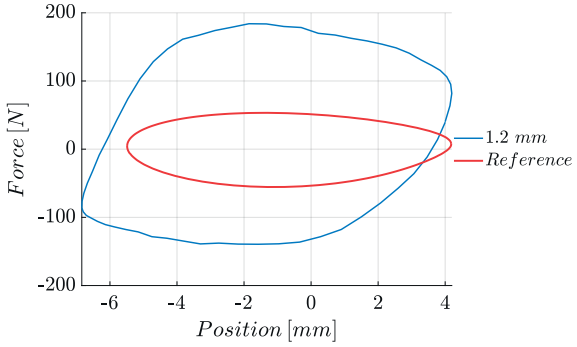

Figure 10 *Power mode force curve of the final model*

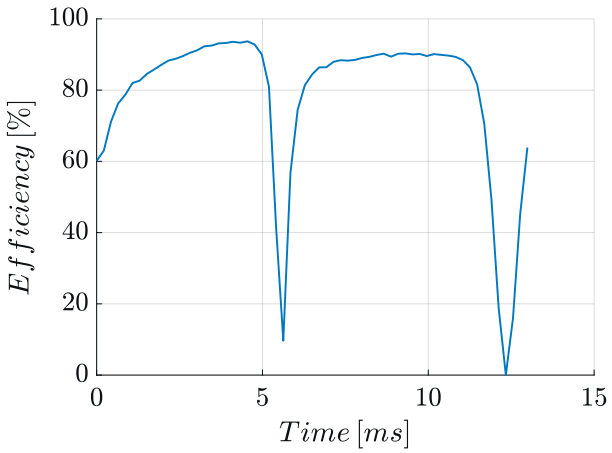

Figure 11 *Efficiency of the efficiency mode during one period*

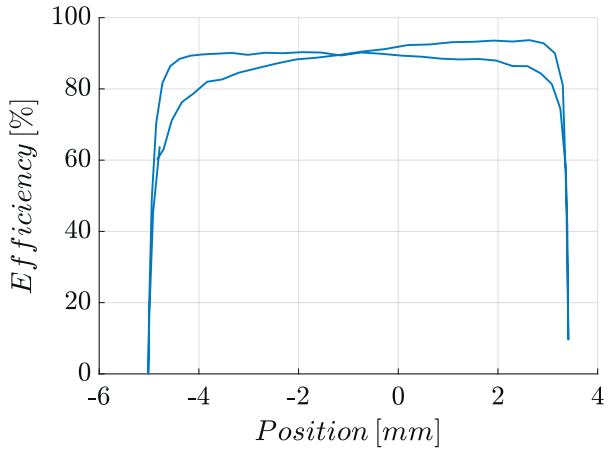

Figure 12 *Efficiency of the efficiency mode during one period for position of the mover*

As previously stated, the SMTLOM with a permanent magnet measuring 1.2 mm in width generates sufficient force to envelop the theoretical force. Despite the initial results exhibiting a reduced number of steps in the simulation, the final model was selected, consequently necessitating a simulation with a greater number of steps. The results for Efficiency mode are available in Figure 9. The Power mode force is visualized in Figure 10.

The produced force, in the efficiency mode, exceeds the theoretical reference throughout the entire movement of the SMTLOM. This indicates that the enhanced simulation precision has led to the elimination of the error that occurred in Figure 8, due to the reduced step size in the simulation.

In the power mode, the force exerted during movement typically exceeds the reference value by a significant margin. It is worth noting that, at its maximum point of movement, the object may not fully cover the reference point. However, this is not necessarily problematic, as the object generates sufficient force during its movement to compress the medium.

With the exception of the efficiency goal, all other objectives were successfully achieved. Therefore, an investigation was conducted into the efficiency of this model. The process of SMTLOM is illustrated in Figure 11.

This phenomenon is more readily apparent in Figure 12, in which the entire movement is displayed.

The maximum achieved efficiency for the efficiency mode during a single periodic movement was 93.692%. According to the operational principle, it is evident that the machine's efficiency will fluctuate. The root mean square (RMS) value of the efficiency is 81.647%. It is imperative to acknowledge that this valuation exclusively encompasses accounts that are associated with electromagnetic efficiency of the standalone linear machine, it does not extend to accounts that incorporate mechanical components. As illustrated in Figures 11 and 12, two significant declines in efficiency are evident, attributable to alterations in direction.

The efficiency of the linear oscillatory machine was evaluated in Ansys Maxwell 3D based on the instantaneous mechanical output power and electromagnetic losses. The instantaneous output power is defined as

$$P_{out}(t) = F(t)\,v(t), \tag{23}$$

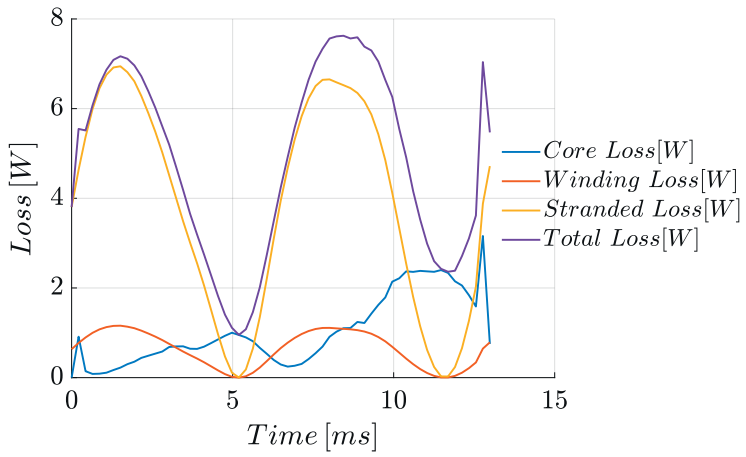

Figure 13 *Losses in the SMTLOM in efficiency mode*

where $F(t)$ is the electromagnetic force acting on the mover and $F(t)$ is its instantaneous velocity. The efficiency is calculated as

$$\eta(t) = \frac{|P_{out}(t)|}{|P_{out}(t)| + P_{loss}(t)} \cdot 100\% . \tag{24}$$

The absolute value of the output power is used due to the oscillatory motion, during which the velocity and power change sign within one period. In this case, the negative power does not represent a loss but a reversal of energy flow. The losses $P_{\text{loss}}(t)$ include only electromagnetic losses of the machine, namely copper and iron losses, while the mechanical and fluid losses are not considered. This efficiency definition is intended for comparative electromagnetic evaluation of different SMTLOM designs and does not represent the overall compressor system efficiency.

In oscillatory systems, such as linear compressors, springs are utilized to maintain resonance. This configuration enables the machine to undergo directional changes with reduced losses, thereby maintaining elevated operational efficiency throughout its function. Therefore, it can be concluded that these substantial declines in efficiency will not be observed in the compressor system. However, some loss of efficiency may still occur in the points during directional changes.

At this stage of the research, the mechanical system had not yet been incorporated into the machine's design. Therefore, it can be concluded that all the figures and values are exclusively applicable to the electromagnetic efficiency of the standalone linear machine. This includes all the forces, which did not take into account weight of the piston and the fluid, the efficiency curves and all the losses. As illustrated in Figure 13, the losses are exclusively those of the machine, excluding any mechanical load. In this particular instance, the greatest proportion of total losses is attributable to stranded losses. The occurrence of stranded losses can result in the heat-related issues, a phenomenon that is characteristic of this particular type of machine. Due to the positioning of the magnets on the exterior surface of the SMTLOM, they are likely to be insulated from elevated temperatures. However, a more comprehensive temperature assessment is necessary to verify this hypothesis.

9 Conclusion

The presented study demonstrates that the proposed SMTLOM is a suitable candidate for driving linear compressors in electric vehicle applications. Through a combination of analytical modelling, 3D finite-element simulations, and multi-stage optimization, the machine was designed to satisfy strict dimensional constraints while achieving the required bidirectional force across the full stroke. The systematic reduction of rare-earth magnet volume, enabled by relocating the magnets to the stator, and employing a transverse-flux topology, proved effective, yielding a final configuration that maintains adequate thrust despite a magnet width of only 1.2 mm. The optimized machine consistently exceeded the theoretical force reference in both efficiency and power modes, confirming that the electromagnetic design is capable of meeting demanding compressor load conditions.

The evaluation of efficiency revealed that, while the instantaneous efficiency varies due to the oscillatory nature of the system, the peak efficiency reaches 93.7%. The efficiency is expected to improve when mechanical springs are included, as resonant operation reduces electrical power demand near reversal points. Losses analysis showed that stranded losses represent the dominant component, highlighting the need for future thermal assessment and potential mitigation strategies. Overall, the results validate the feasibility of the SMTLOM concept and establish a solid foundation for future work involving mechanical integration, thermal modelling, and prototype development.

Acknowledgment

The authors would like to thank BSH Drives and Pumps s.r.o. for their support during this research. This research was funded by the Slovak Research and Development Agency APVV No. DS-FR-24-0056 and KEGA K-25-010-00.

Conflicts of interest

The authors declare that they have no known competing financial interests or personal relationships that could have appeared to influence the work reported in this paper.

References

[1] ZHANG, Z., WANG, J., FENG, X., Chang, L., Chen, Y., Wang, X. The solutions to electric vehicle air conditioning systems: a review. *Renewable and Sustainable Energy Reviews* [online]. 2018, **91**, p. 443-463. ISSN 1364-0321, eISSN 1879-0690. Available from: https://doi.org/10.1016/j.rser.2018.04.005

[2] ZHANG, Z., WANG, D., ZHANG, CH., CHEN, J. Electric vehicle range extension strategies based on improved AC system in cold climate - a review. *International Journal of Refrigeration* [online]. 2018, **88**, p. 141-150. ISSN 0140-7007, eISSN 1879-2081. Available from: https://doi.org/10.1016/j.ijrefrig.2017.12.018

[3] KIM, S.-I., LEE, G.-H., HONG, J.P., JUNG, T.-U. Design process of interior PM synchronous motor for 42-V electric air-conditioner system in hybrid electric vehicle. *IEEE Transactions on Magnetics* [online]. 2008, **44**(6), p. 1590-1593. ISSN 0018-9464, eISSN 1941-0069. Available from: https://doi.org/10.1109/TMAG.2007.916136

[4] JUNG, T.-U., LEE, S.-H., KIM, S.-I., PARK, S.-J., HONG, J.-P. The development of hybrid electric compressor motor drive system for HEV. In: 2007 IEEE Vehicle Power and Propulsion Conference: proceedings [online]. IEEE. 2007. ISSN 1938-8756, ISBN 978-0-7803-9760-6, p. 802-807. Available from: https://doi.org/10.1109/VPPC.2007.4544234

[5] XUE, X., CHENG, K. W. E., ZHANG, Z. Model, analysis, and application of tubular linear switched reluctance actuator for linear compressors. *IEEE Transactions on Industrial Electronics* [online]. 2018, **65**(12), p. 9863-9872. ISSN 0278-0046, eISSN 1557-9948. Available from: https://doi.org/10.1109/TIE.2018.2818638

[6] ZHANG, Y., LU, Q., YU, M., YE, Y. A novel transverse-flux moving-magnet linear oscillatory actuator. *IEEE Transactions on Magnetics* [online]. 2012, **48**(5), p. 1856-1862. ISSN 0018-9464, eISSN 1941-0069. Available from: https://doi.org/10.1109/TMAG.2011.2178077

[7] BOLDEA, I., NASAR, S.A., PENSWICK, B., ROSS, B., OLAN, R. New linear reciprocating machine with stationary permanent magnets. In: IAS '96. Conference Record of the 1996 IEEE Industry Applications Conference Thirty-First IAS Annual Meeting: proceedings [online]. Vol. 2. 1996. ISSN 0197-2618, ISBN 0-7803-3544-9, p. 825-829. Available from: https://doi.org/10.1109/IAS.1996.560179

[8] LI, X., XU, W., LIAO, K., WU, X. Design of stator-magnet moving-iron transverse-flux linear oscillatory machine considering asymmetric saturation. *IEEE Transactions on Transportation Electrification* [online]. 2022, **8**(3), p. 3464-3477. eISSN 2332-7782. Available from: https://doi.org/10.1109/TTE.2022.3152909

[9] LI, X., JIANG, M., XU, W., WU, T., ZHANG, D. Design and test of a less-rare-earth stator-magnet moving-iron transverse-flux linear oscillatory machine for reciprocating drive. *IEEE Transactions on Industrial Electronics* [online]. 2024, **71**(3), p. 2831-2841. ISSN 0278-0046, eISSN 1557-9948. Available from: https://doi.org/10.1109/TIE.2023.3269472